Journal of Paleolithic Archaeology (2025) 8:12
https://doi.org/10.1007/s41982-025-00213-6

RESEARCH

Archaeomagnetic Tools Applied to the Study of Middle Palaeolithic Hearths: The Level R (*ca.* 60 ka BP) at Abric Romaní (NE Iberian Peninsula)

Judit del Río[1] · Alicia Palencia-Ortas[2] · Miriam Gómez-Paccard[3] · Ángel Carrancho[1] · Palmira Saladié[4,5,6] · M. Gema Chacón[4,5,7] · Eudald Carbonell[4,5] · Josep Vallverdú[4,5,6]

Accepted: 28 February 2025

Abstract
Due to its long occupation throughout the Middle Palaeolithic and the abundance of its pyrotechnological evidence, the Abric Romaní rockshelter (Capellades, Barcelona) provides an ideal setting for studying Neanderthal fire use. We conducted an archaeomagnetic study of four hearths from Level R (*ca.* 60 ky BP). Rock magnetism experiments, including hysteresis loops, and backfield, isothermal remanent magnetisation acquisition and thermo-magnetic curves, were conducted on three specimens per hearth to investigate their magnetic mineralogy. To explore the raw material's ability to become magnetised, we performed a laboratory-induced partial thermo-remanent magnetisation acquisition in a 50μT field at various increasing temperatures. Our results indicate that the material is predominantly diamagnetic, but contains a small proportion of low coercivity magnetic minerals, likely magnetite. A total of 106 oriented specimens underwent progressive thermal demagnetisation up to 580 °C. Directional results at the specimen level show either a single component or two: one between 250 and 420 °C and another between 300 and 550 °C. Three out of the four hearths yielded normal-polarity archaeomagnetic directions, within the range of secular variation expected for their estimated age; the poor quality of the data prevented any analysis of the remaining structure. These findings suggest that, despite the hearths' low content in ferromagnetic minerals, they are able to acquire a thermal or thermochemical-remanent magnetisation, accurately recording the Earth's magnetic field though their high-temperature component. The low-temperature component may reflect a subsequent thermo-chemical or chemical alteration that partially remagnetised the original direction.

Keywords Archaeomagnetism · Hearths · Middle Palaeolithic · Neanderthals · Iberian Peninsula

Introduction

The aim of the present study is the magnetic characterisation of four Middle Palaeolithic hearths sampled at the level R (*ca.* 60 ka BP) of the Abric Romaní, a prehistoric rock shelter with Middle Palaeolithic occupation levels that span roughly between 70 and 40 ka BP (Sharp et al., 2016). The term *hearth* refers, throughout the literature about prehistoric archaeology, to a *fireplace* or *combustion structure*, or a surface where a fire has been burning, together with

✉ Judit del Río
jdelrio@ubu.es

[1] Dpto. Historia, Geografía y Comunicación – Área de Prehistoria, Universidad de Burgos, Pza. Misael Bañuelos García s/n, 09001 Burgos, Spain

[2] Dpto. Ingeniería Eléctrica, Electrónica Automática y Física Aplicada, Universidad Politécnica de Madrid - E.T.S. de Ingeniería y Diseño Industrial, Ronda de Valencia 3, 28012 Madrid, Spain

[3] IGEO, Instituto de Geociencias (CSIC-UCM), C/ Dr. Severo Ochoa 7, 28040 Madrid, Spain

[4] Institut Català de Paleoecologia Humana I Evolució Social, IPHES-CERCA, Zona Educacional 4, Campus Sescelades URV, Edifici W3, 43007 Tarragona, Spain

[5] Dpt. Història I Història de L'Art, Universitat Rovira I Virgili, Avda. de Catalunya 35, 43002 Tarragona, Spain

[6] Unit Associated with CSIC, Department of Paleobiology, National Museum of Natural Sciences, Madrid, Spain

[7] UMR7194 – Histoire naturelle de l'Homme préhistorique (CNRS – MNHN – UPVD – Sorbonne Université), Musée de L'Homme, 17 Place du Trocadéro, 5016 Paris, France

Published online: 28 March 2025

its remnants (Mallol et al., 2017). Hearths are deemed an important finding at a site, as they serve as evidence of pyrotechnology: the use of fire by prehistoric societies.

The ability to control fire is particularly relevant in archaeological research, as it is considered one of the main technological achievements that substantially modified human behaviour and habitat (Aldeias et al., 2016; Allué et al., 2022; Brown et al., 2009; Dibble et al., 2018; Sandgathe et al., 2011). This work makes use of the traces left by Neanderthal fire technology in the archaeological record to retrieve information about the temperatures these fires reached, and how the population used their habitat. Additionally, it aims to describe the Earth's magnetic field behaviour in past times, thus positioning the research within the field of archaeomagnetism.

Archaeomagnetism is the discipline that studies the magnetic properties of certain archaeological materials (Néel, 1949, 1955; Thellier, 1951; Thellier & Thellier, 1941, 1959). Its fundamentals rely on the ability of some iron-rich minerals, particularly iron oxides and hydroxides, to acquire a thermo-remanent magnetisation (TRM): a permanent state of magnetisation that remains stable over time. This occurs when these ferromagnetic (*sensu lato*) minerals are heated above a certain temperature and then cool in an ambient field —in this case, the Earth's magnetic field. These minerals, acting like a compass within the archaeological burned material, freeze in the direction of the field in which they cool. This direction is typically defined by the magnetic declination and inclination values, which vary both spatially and temporally at different time scales, from decadal to millennial. This variation is known as palaeosecular variation. For further details on how archaeological materials become magnetised, see Schmidt (2007), Tarling (2007), or Tauxe et al. (2018).

Archaeomagnetic studies can serve various purposes (Gallet et al., 2009). They can be used to date archaeological materials (Le Goff et al., 2002; Pavón-Carrasco et al., 2011), decipher the formation of the archaeological record—such as soil disturbance, land movements due to human or animal activity that are not immediately apparent (Bradák et al., 2021; Kapper et al., 2014), or the presence of invisible fire features in archaeological levels (Mallol et al. 2019). As such, archaeomagnetism has significantly contributed to enhancing our understanding of various archaeological sites (Gómez-Paccard et al., 2019; Stillinger et al., 2018). Additionally, archaeomagnetism can be applied to independently dated archaeological materials to extract information about the Earth's past magnetic field by constructing regional palaeosecular variation curves or regional and global geomagnetic field models (Campuzano et al., 2019; Carrancho et al., 2013; Bonilla-Alba et al., 2021, 2024). A more refined knowledge of geomagnetic field variations leads to more accurate models, which, in turn, improve archaeomagnetic dating accuracy. Consequently, one of the main objectives of archaeomagnetism is to fully characterise the geomagnetic field of the past, constantly invested in expanding its spatial and temporal database (Brown et al., 2021).

Archaeomagnetic research has traditionally been conducted on well-burned archaeological findings such as furnaces, ovens, pottery kilns, and accidentally burned walls. There is, however, a growing body of research exploring previously overlooked materials, such as burned chert or sediments (Carrancho et al., 2013; Herrejón-Lagunilla et al., 2022; Kapper et al., 2015; Zeigen et al., 2019). This new assortment of materials opens up new possibilities for the discipline, particularly in terms of extending the temporal scope of our studies. With older samples comes an increased knowledge about the magnetic field in the distant past, and the promises of better resolution for geomagnetic field models are enticing.

These novel developments have allowed prehistoric archaeomagnetism to gain momentum, as evidenced by an increasing number of studies in Palaeolithic sites (e.g. Álvarez-Fernández et al., 2018; Bradák et al., 2021; Dinçkal et al., 2024; Herrejón-Lagunilla et al., 2024; Leierer et al., 2020). The number of such studies grows even more when we cross the Holocene boundary (e.g. Carrancho et al., 2009; Di Chiara et al., 2021; Kapper et al., 2014; Kostadinova-Avramova et al., 2020; Palencia-Ortas et al., 2021; Wang et al., 2023; the references here are not intended to be an exhaustive, but rather to highlight some recent works). The quantitative asymmetry in research can, in part, be explained by the availability (or lack thereof) of pyrotechnology throughout human history.

The Abric Romaní's infill comprises an archaeological sequence of approximately 20 m of sediments, with 20 archaeological levels identified to date. This impressive archaeological record encompasses thousands of lithic artefacts, as well as faunal and palaeobotanical remains. The site is known for its significance in the study of prehistoric fire, with over 200 combustion activity areas excavated (Vallverdú et al., 2010; Vallverdú et al., 2012b). Some of these structures have been the subject of previous archaeomagnetic research. Specifically, Carrancho et al. (2016) presented the magnetic properties of three Middle Palaeolithic hearths from the younger Level O (*ca.* 55 ky BP) and discussed the role of archaeomagnetism in palimpsest dissection—a palimpsest being the overlapping of different features in the archaeological record in such a way that they cannot be readily identified nor their chronologies attested, at least *de visu* (Bailey, 2007). Building upon that work, we present here a new archaeomagnetic study of four combustion structures sampled in the level R of Abric Romaní (*ca.* 60 ky BP).

The aims of this study are as follows: (a) to identify different occupation events based on the archaeomagnetic directional record preserved in the combustion features;

(b) to obtain information about the technological processes related to fire-making, specifically the minimum temperatures reached by each hearth; (c) to evaluate whether the taphonomic processes involved in the formation of the archaeological record affect the archaeomagnetic directions.

Geological and Archaeological Setting

Location

The Abric Romaní is a travertinic rockshelter, one amongst many in the karstic system known locally as *Cinglera del Capelló*. Located in Capellades, Barcelona (1°41′30″ E, 41°32′00″ N), in the Anoia river valley at an elevation of 265 m.a.s.l. (Fig. 1A), the site has seen a long history of archaeological research since its beginning in 1909. The current excavations, led by a team at IPHES (Catalan Institute of Human Paleoecology and Social Evolution), focus on the systematic retrieval and documentation of archaeological findings, including a significant number of combustion structures. Area excavations provide insight into the settlement's size and distribution, revealing settlement dynamics inside the shelter. The *Cinglera del Capelló* is built of calcareous tufa, deposited by the action of the local springs of the Carme-Capellades aquifer. The Abric Romaní's infill comprises these calcareous tufas and clastic tufa sediments (Fig. 1C). A detailed description of the shelter's lithofacies and sedimentary sequences can be found in Vallverdú (2018) and Vallverdú et al. (2012b).

The Archaeological Level R

The current chronostratigraphy of the rockshelter is based on U-series and radiocarbon analyses (Bischoff et al., 1988; Vaquero et al., 2013). Recent core sampling has revealed levels extending up to 30 m below the current excavation surface, suggesting the site was occupied as early as 110 ka ago (Sharp et al., 2016). The excavation of level R began in 2018 and consists of several sub-levels (Fig. 1C). The first, the superficial sub-level *Rsup* (superior), revealed numerous hearths and ample evidence of wood use. Sub-level *Ra* appears directly below it and is located mainly towards the interior wall of the shelter and less rich in findings. Sub-level *Rb* is the oldest horizon and is currently being excavated. All three of them are relatively thin layers (IPHES—Institut Català de Paleoecologia Humana i Evolució Social, 2020, 2021, 2022). Level R as a whole is dated to *ca.* 60 ka BP (Bischoff et al., 1988; Sharp et al., 2016).

Most of the materials for our study were sourced from the sub-level *Rest* (structural). This classification refers to findings that cannot be precisely attributed to any of the aforementioned sub-levels or layers within the larger Level R deposit (Fig. 1C). The precise attribution of these findings (whether to Rsup, Ra, or Rb) will depend on the careful analysis of their microstratigraphy, taking into account the entire record for the level and integrating all available archaeological data.

Combustion Structures at Abric Romaní

The pyro-technological record at Abric Romaní has been the focus of several studies, from the early reports of the hearths of Level J by Vallverdú (2002) to the more recent studies of newer levels (Vallverdú et al., 2012a, 2012b). These studies have provided evidence that links the combustion structures at the site with the analysis of activity areas within the shelter (Allué et al., 2012; Courty et al., 2012; Pastó et al., 2000; Téllez et al., 2022; Vallverdú et al., 2005, 2010,¡; Vallverdú et al., 2012b; Vallverdú & Courty, 2012; Vaquero & Pastó, 2001).

These combustion structures are identified in situ during excavation as blackened areas on the surface of the archaeological level (Fig. 1B). Their systematic micro-stratigraphic structure was first recorded in the hearths unearthed in level N (Vallverdú et al., 2010), and was later identified in older levels, including level O (Carrancho et al., 2016). Said structure is comprised by the uppermost carbonaceous layer—a dark deposit whose colour is related to charcoal-rich sediments—and the underlaying rubefied layer—reddened by thermal alteration, usually displaying a convex, lenticular shape, and a smaller area than the black carbonaceous layer. These two upper layers, the direct outcome of human fire use upon the rockshelter's floor, measure only 2–4 cm in depth. Below them lies the unaltered substrate, which is pale yellow and shares the vacuolar structure of the calcareous tufa sedimented in the shelter. The hearths selected for this study share this same stratigraphy, and they will be characterised in more detail in the following section.

Materials and Sampling

All the materials for this study were collected during the 2021 field campaign. They consist of a total of four hearths from the archaeological level R (described in the 'Combustion Structures at Abric Romaní' section and shown in Figs. 1 and 2), which were retrieved from the field in blocks, or field samples, by means of the plaster cap technique (Thellier, 1981). The process is as follows: first, an artificial horizontal surface is created upon the hearth (by pouring liquid plaster, which is levelled before it sets with a methacrylate plate and a bulls-eye spirit). Once dry, the sample is oriented by marking the direction of the current magnetic north on the surface with the aid of a magnetic compass and then extracted (Fig. 2C and E). Although the

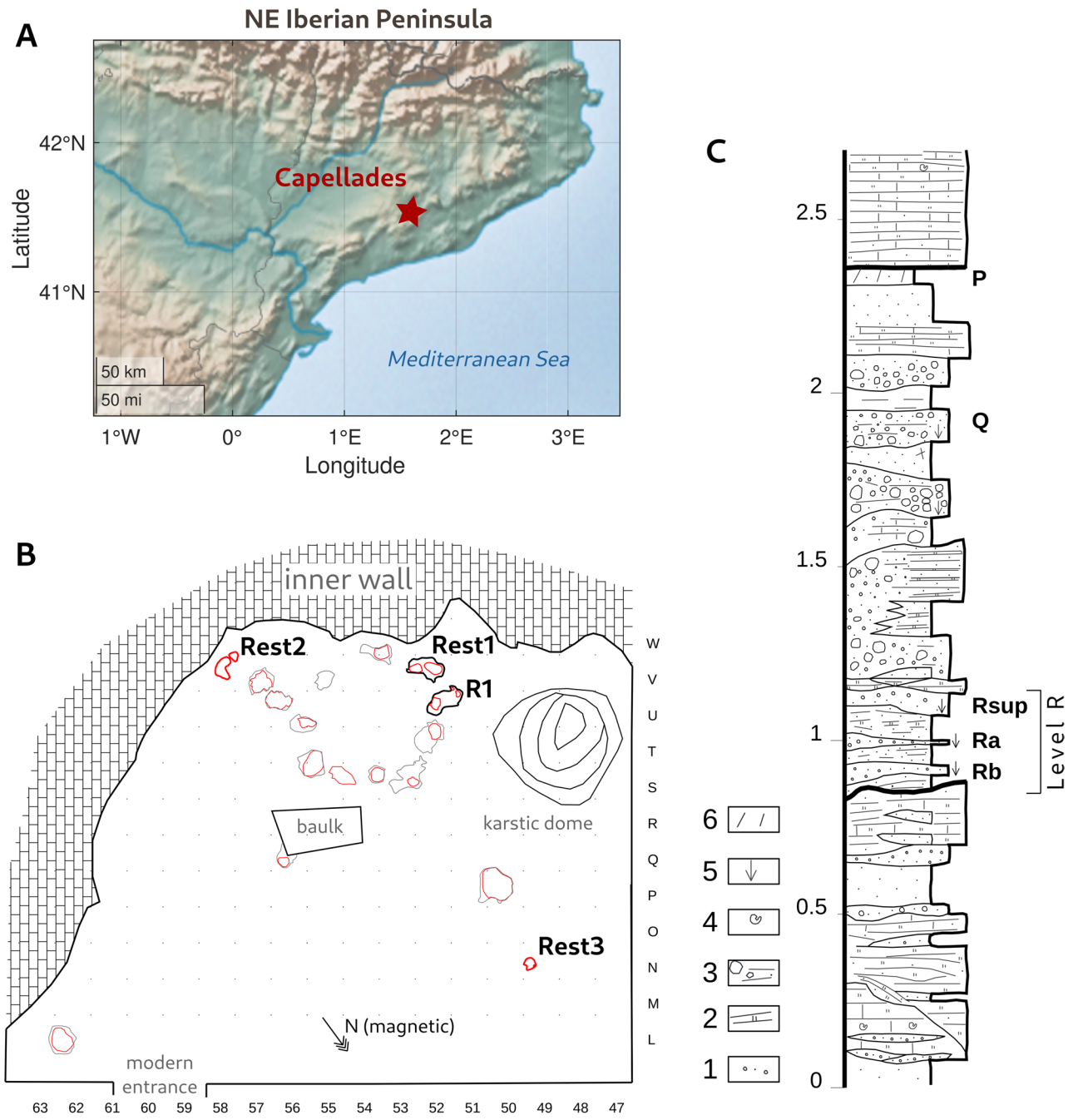

Fig. 1 **A** Location of the Abric Romaní at Capellades, NE of the Iberian Peninsula; **B** planimmetry of the rockshelter's Level R, showing the studied hearths in bold amongst other similar structures—black lines define the carbonaceous facies, red lines the rubefied facies. Note that not all hearths found at Level R are depicted for clarity, and that each square in the grid is 1 × 1 m; **C** stratigraphic sequence based on column 47's profile, showing the lithostratigraphy of the archaeological levels P, Q, and R. Legend in (**C**): 1, sandy tufa fine gravels; 2, sandy phytoclasts in thin horizontal laminae; 3, sandy tufa coarse gravels in thick horizontal discontinuous laminae; 4, criptokarst; 5, inverse grading; 6, organomineral dark mud (palaeosol/organic horizon epipedon)

solar compass is preferred due to its increased accuracy in azymuthal orientation, the conditions of the site, which lacks sunlight, prevented its use in this case.

The hearths for this study belong to two sub-levels: Level R (general, nondescript) and Level Rest (structural), with the hearths named accordingly. Hearth *R1* belongs to Level R and has four oriented samples, whilst hearths *Rest1* (four

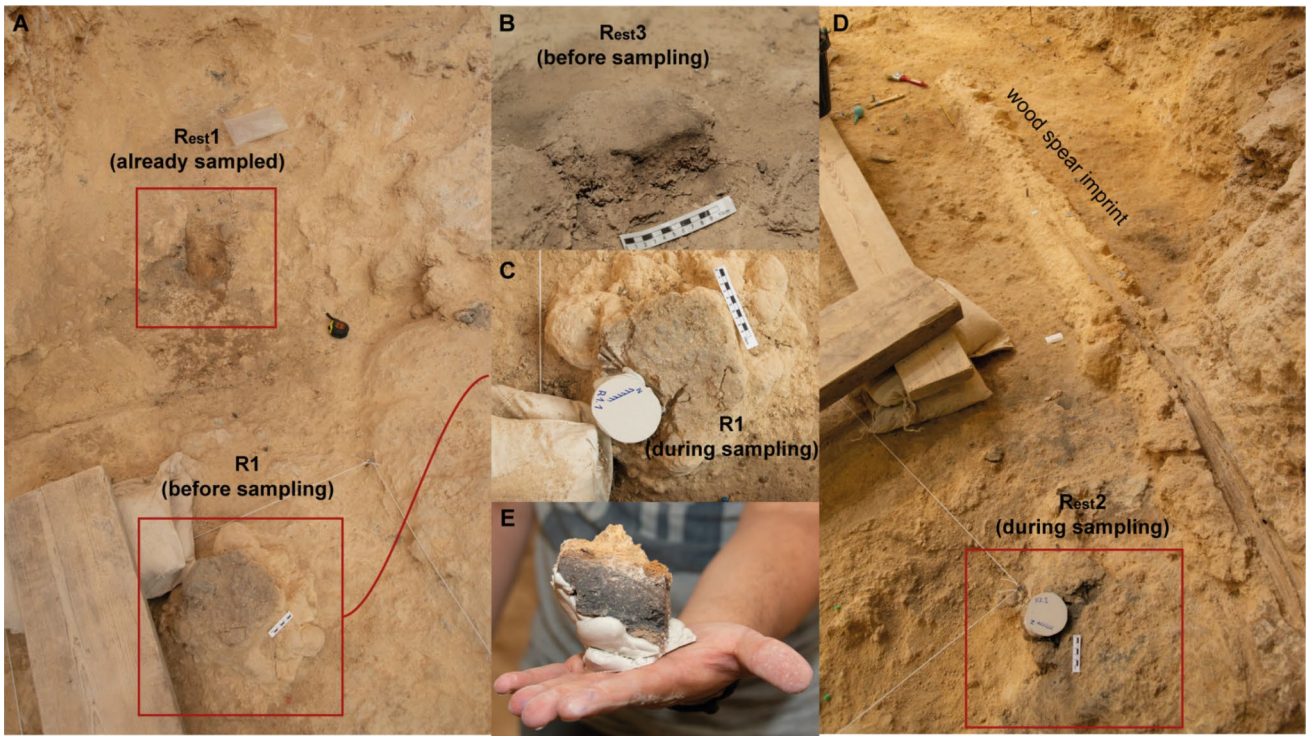

Fig. 2 **A** General view of hearth R1 (before being sampled) and hearth Rest1 (already retrieved); **B** close-up of hearth Rest3 before sampling; **C** close-up of hearth R1 during sampling, with the azimuth line drawn on the surface; **D** general view of hearth Rest2 during sampling; it lays near a well-preserved wood imprint; **E** one of the hand samples blocks after extraction, shown upside down, with the carbonaceous black layer can be seen

oriented samples), *Rest3* (six oriented samples), and *Rest4* (three oriented samples) belong, accordingly, to Level Rest. The number of blocks retrieved varies depending on the size of the hearth and its characteristics, such as friability or cementation. In addition, non-oriented bulk samples were collected from the carbonaceous layers in hearths *Rest1* and *Rest2*, as well as from the neighbouring unburned substrate, to be used in rock magnetism experiments (Fig. 2).

At their arrival at the laboratory, the samples were consolidated in a 60% solution of sodium silicate, embedded in a prismatic plaster mould, and then cut into 2-cm side slices and 8 cm^3 cubic specimens, preserving the orientation lines. Further consolidation with a 75% sodium silicate solution was applied in between cutting stages as needed, depending on the fragility of the materials, which are, for the most part, very porous and friable.

During laboratory work, photographs of the cross-cut sections of each field sample were taken (Fig. 3). Archaeomagnetic sub-sampling destroys the hearth's morphology, making it difficult to visualise their original appearance. The visual record can prove vital in later stages, when interpreting the results. Differences in appearance between the hearths are notable, as is the variability in depth in each of them. In *R1*, the darkened upper layer rests atop a lighter substrate (Fig. 3A). In *Rest1*, the surface dips, with the carbonaceous layer interrupted by a white calcareous wedge, possibly related to a secondary deposition, and a clear boundary with the underlying substrate (Fig. 3B). *Rest2* shows a thick carbonaceous layer, not completely horizontal and overlain by a calcareous patina on the uppermost millimetres; this facies transitions into a rubefied brownish substrate (Fig. 3C). *Rest3*, by contrast, has minimal darkening of the upper layer, and the vacuolar structure of the calcareous substrate is more pronounced (Fig. 3D).

Experimental Setup

Rock Magnetism

The natural remanent magnetisation (NRM) of all 106 specimens was measured using a helium-operating SRM 755 cryogenic magnetometer (2G Enterprises). Room-temperature magnetic susceptibility was measured prior to thermal treatment with a KLY-4S Kappabridge meter paired with its pick-up unit (AGICO). In some specimens, the magnetic susceptibility was routinely checked after each temperature increase to monitor potential mineralogical changes due to heating.

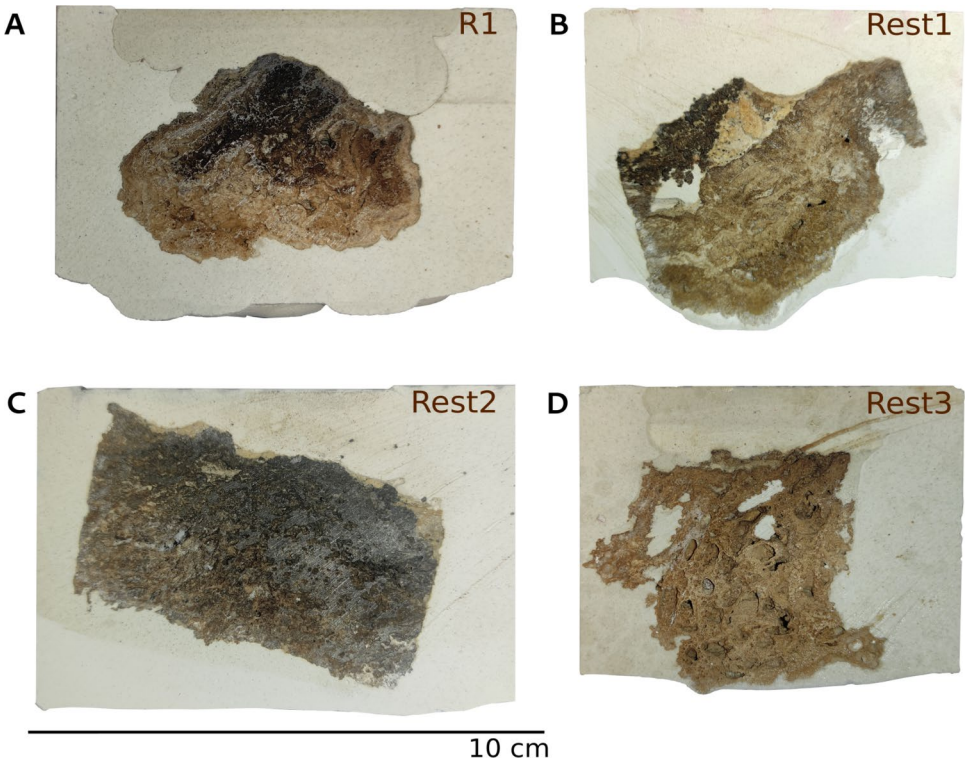

Fig. 3 An assortment of materials used in this study, with representative cross-sections of samples from all four hearths taken during laboratory subsampling: **A** R1; **B** Rest1; **C** Rest2; **D** Rest3

We then conducted a rock magnetic characterisation of each combustion structure (three specimens per hearth), which included a standard set of experiments: an isothermal remanent magnetisation (IRM) acquisition curve in 15 steps up to 1000 mT, a hysteresis loop (±900 mT), a backfield curve (−900 mT), and a magnetisation vs. temperature thermo-magnetic curve in air up to 700 °C and back to room temperature again. These experiments help to identify the nature, concentration, and domain-state of the magnetic carriers in the specimens. Specifically, IRM acquisition helps determine the field at which the specimen reaches saturation magnetisation, allowing us to distinguish between low and high coercivity magnetic minerals. Thermo-magnetic curves are used to estimate the Curie temperatures, which are specific to every different iron oxide. We calculated the Curie temperatures using the second derivative, though in some cases significant noise due to the low magnetic signal and/or a nearly linear curve prevented this—we used Moskowitz's (1981) method in these cases. The shape of the curve also helps to detect mineralogical changes during heating by comparing the similarity (reversibility) between the heating and cooling branches of the experiment. Hysteresis and backfield curves provide magnetic parameters such as saturation magnetisation (*M*s), saturation remanent magnetisation (*M*rs), coercive field (*H*c), and remanent coercive field (*H*cr). These values were obtained after correcting the hysteresis loop for paramagnetic and diamagnetic contributions. All measurements were performed in a Variable Field Translation Balance (Mag Instruments), and we used RockMagAnalyzer v.01 (Leonhardt, 2006) for our data analysis.

An ancillary Lowrie test, or thermal demagnetisation of the IRM (Lowrie, 1990), was also performed on four representative specimens, one per hearth. Fields of 2 T ('hard', high-coercivity component), 400 mT (medium-coercivity component), and 120 mT ('soft', low-coercivity component) were induced in all three orthogonal axes (*x*, *y*, *z*). Thermal demagnetisation was then performed between room temperature and 600 °C in 12 steps, with the temperature increase in each step varying between 50 and 30 °C, using a TD48-DC double chamber thermal demagnetiser (ASC Scientific). Fields were induced with an IM-10–30 impulse magnetiser (ASC Scientific), and remanent magnetisations were measured in the same magnetometer mentioned above.

Substrate Characterisation: Simulation of TRM Acquisition in Unburned Substrate Specimens

Further tests were carried out to fully characterise the calcareous substrate atop which the hearths were lit. Our aim was to assess the suitability of the Abric Romaní's karstic infill for acquiring a stable thermoremanent magnetisation (TRM) under heating conditions. A secondary goal was to determine the temperature at which the unburned specimens acquire a TRM, identifying when their NRM intensity

reaches similar values to those observed in the demagnetised hearth samples (heated during the Palaeolithic).

For these experiments, we selected four specimens (one per hearth) of unburned substrate from the lower layers (2–4 cm in depth). After measuring their NRM and magnetic susceptibility at room temperature, we performed a laboratory-induced pTRM acquisition in a field of 50 μT along all three orthogonal axes at different temperatures in the following sequence: (1) TRM acquisition along the -*z* axis at 500 °C, (2) increasing partial TRM (pTRM) acquisition along the -*y* axis at 400 °C, 450 °C, and again at 500 °C, and (3) pTRM acquisition along the -*x* axis at 350 °C.

The TRM acquisition experiments were carried out using an MMTD80A thermal demagnetiser (Magnetic Measurements), coupled with a Tti EL302 power supply unit. After each heating step, the remanence was measured for each specimen using the cryogenic magnetometer. Additionally, magnetic susceptibility (χ) was measured before and after the initial high-temperature heating at 500 °C to assess any variation. This was later compared to the variation in susceptibility before and after thermal treatment in the specimens from the same hearth used in thermal demagnetisation experiments.

Thermal Demagnetisation of the NRM

A total of 106 specimens underwent stepwise thermal demagnetisation in the TD48-DC oven, with the primary aim of determining the direction of the characteristic remanent magnetisation (ChRM) in each specimen. Thermal demagnetisation was preferred over alternating field (AF) demagnetisation due to its effectiveness in defining archaeomagnetic components and providing information about the last heating temperature reached by the burned materials (Francés-Negro et al., 2019). The demagnetisation was conducted in two phases. The first batch of 32 specimens (8 per hearth) was demagnetised in 20 °C steps up to 580 °C. The remaining 74 specimens (originally 20 per hearth, but six were broken during heating and/or manipulation) in the main experiment were demagnetised in 50 °C steps up to 200 °C, and in 30 °C steps up to 580 °C. After each step, the remanent magnetisation was measured using the SRM 755 magnetometer.

All specimen preparation and measurements described in this section were carried out at the PALEOMAG-UBU facilities (University of Burgos). We analysed the directional data with Remasoft 3.1 (Chadima & Hrouda, 2006), calculating the declination and inclination values at the specimen level with their associated maximum angular deviation (MAD) (Kirschvink, 1980). Directions were averaged by hearth, and statistical parameters were calculated assuming a Fisherian distribution (Fisher, 1953), including the precision parameter k and the $\alpha 95$ (95% cone of confidence), as is standard in archaeomagnetic studies.

Results

Rock Magnetism and Magnetic Mineralogy

The measurements of mass-normalised magnetic susceptibility (χ) before heating reveal two groups of specimens: the first with negative susceptibility values (minimum value = −3.85E−09 m^3/kg), and the second with low positive values (max. value = 2.92E−08 m^3/kg). Negative susceptibilities are expected in diamagnetic materials (as is the carbonate of the substrate), and the overall results indicate that the content of ferromagnetic minerals in the samples is very low. Figure 4A shows the normalised mass magnetic susceptibility of all specimens before thermal treatment, showing that the selected specimens' susceptibility values (red dots) are similar to those of the rejected ones (grey dots, with anomalous NRM directions). NRM intensities range from 1.09E−07 to 1.68E−06 Am^2/kg (in Fig. 4B, plotted against χ). Note that the typical Koenigsberger (1930) ratio graph is logarithmic in scale and not suitable for negative susceptibilities; as such, this is not a Qn plot per se, although it follows the same principle and aims to explore the correlation between NRM and magnetic susceptibility, if any. We were not able to use susceptibility as an indicator of the adequacy of the specimens for experimental purposes—i.e. specimens with higher and lower susceptibilities behaved similarly during thermal demagnetisation.

The IRM acquisition (Fig. 4C) and backfield (not shown) curves display similar results for all hearths, withy moderately to very noisy curves, as expected due to the low content of ferromagnetic minerals present in our samples. Saturation is reached at low magnetic fields (< 200 mT), and the samples exhibit small coercive fields, up to 15 mT—the magnetic carrier being a very low coercivity magnetic mineral.

The hysteresis loops exhibit a clear diamagnetic behaviour before its correction (Fig. 4D'), in accordance with the negative or very low susceptibility values reported above. In some cases and only after removing the diamagnetic contribution, hysteresis loops show non-constricted loops that saturate at approximately 100 mT. Thermo-magnetic curves are mostly reversible in specimens from hearths R1, Rest1 and Rest2 (Fig. 4E), and non-reversible in some specimens from hearth Rest3 (Fig. 4F). In all cases, the Curie temperatures range between 470 and 620 °C. The Lowrie test (Fig. 4G) confirms these observations, showing that most of the magnetisation is acquired along the axis where a 120-mT field was induced (the 'soft', low-coercivity component). This magnetisation is completely removed at temperatures between 550 and 600 °C.

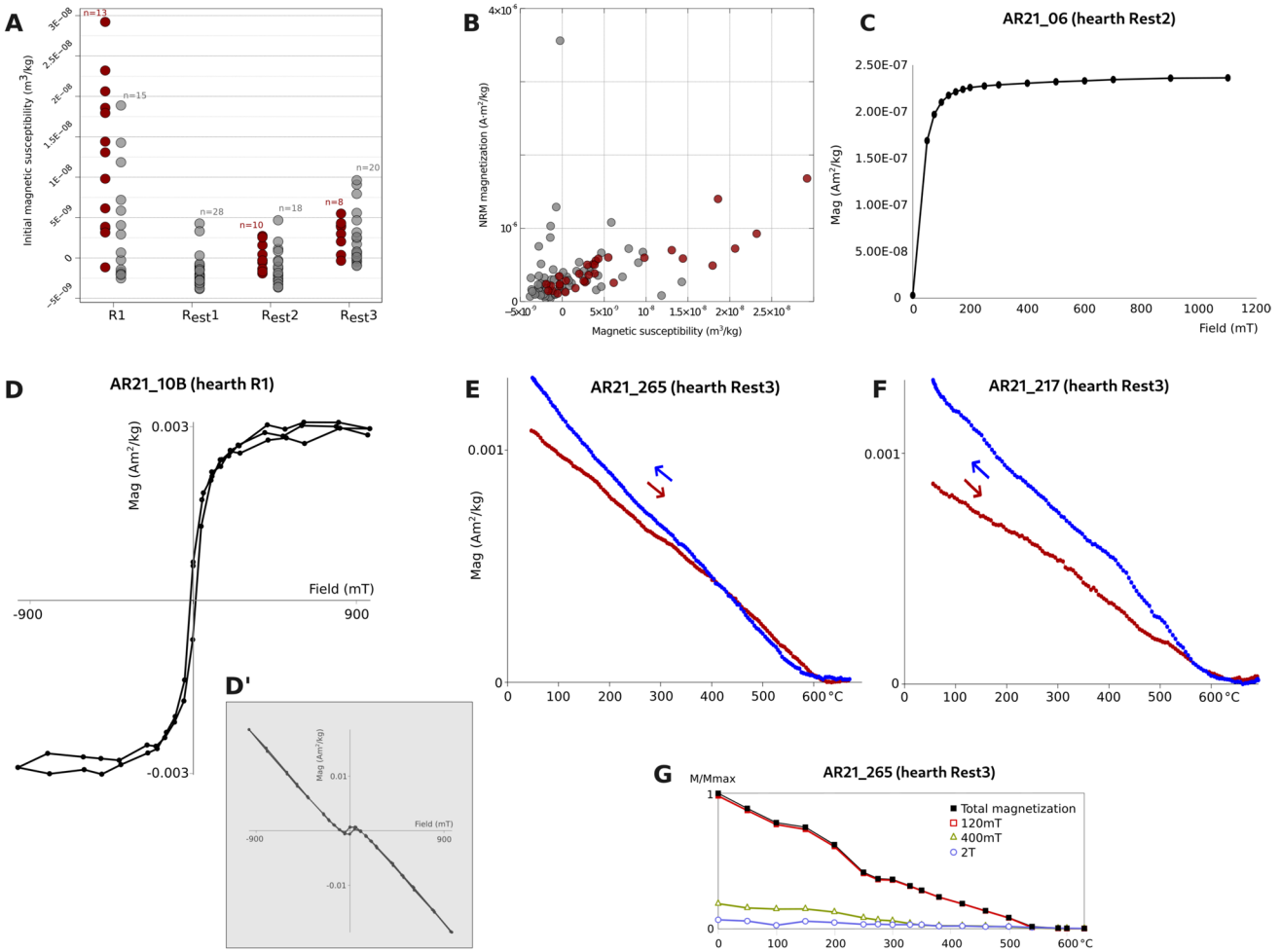

Fig. 4 Results of representative rock magnetism experiments. **A** Mass magnetic susceptibility for all studied specimens, measured before any thermal treatment: red points depict specimens later used for directional analysis, grey points specimens that were rejected (notice that the susceptibility of selected vs. rejected specimens does not vary significantly between both groups); **B** NRM vs. mass magnetic susceptibility for all specimens, showing that a great number display negative values for the susceptibility variable. **C** IRM acquisition curve; **D** hysteresis loop after the subtraction of the para- and diamagnetic fraction; D' uncorrected hysteresis—note the highly diamagnetic shape; **E** reversible magnetisation vs. temperature curve; **F** irreversible magnetisation vs. temperature curve; **G** Lowrie test showing that the soft component (120 mT) contributes most of the magnetisation. All plots are representative of all studied hearths, as the magnetic mineralogy is very homogeneous

Table 1 Rock-magnetic parameters for the Level R hearths. *S*, saturation at 300 mT; *Bcr*, remanent coercive field; *Ms*, saturation magnetisation; *Mrs*, remanent saturation magnetisation; *Bc*, coercive field; T_C, Curie temperature

Hearth	Specimen	S	Bcr (mT)	Ms (Am^2/kg)	Mrs (Am^2/kg)	Bc (mT)	Mrs/Ms	Bcr/Bc	T_C (°C)
R1	10	0.93	31.02	2.48E−03	3.68E−04	12.81	0.15	2.42	584
	033_dark	1.01	26.68	1.75E−03	2.96E−04	12.54	0.17	2.13	627
	033_light	1.01	24.68	1.32E−03	2.17E−04	23.58	0.16	1.05	598
Rest1	98	1.07	39.09	6.44E−04	1.91E−04	17.67	0.30	2.21	563
	113	0.95	33.21	7.25E−04	1.73E−04	15.66	0.24	2.12	548
	126	1	33.59	5.66E−04	1.61E−04	16.64	0.28	2.02	617
Rest2	143	1.01	39.09	7.52E−04	1.22E−04	15.79	0.16	2.48	––
	186	0.96	35.41	6.00E−04	1.22E−04	13.39	0.20	2.64	586
	209	0.96	28.8	1.28E−03	1.98E−04	13.02	0.15	2.21	603
Rest3	217	0.98	18.84	1.37E−03	2.58E−04	13.74	0.19	1.37	597
	239	0.93	32.94	1.49E−03	1.67E−04	8.15	0.11	4.04	445
	257	1.12	28.21	1.15E−03	1.89E−04	12.61	0.16	2.24	649

Overall, the combined analysis of all rock-magnetic results (low saturation and coercive fields, and Curie temperatures between 500 and 600 °C or slightly higher; Table 1) suggests that the main carrier of magnetisation is magnetite or slightly oxidised (maghemitised) magnetite, albeit in small quantities.

Suitability of Level R Materials for Acquiring a TRM

Figure 5 shows the laboratory-induced partial thermoremanent magnetisation (pTRMs) acquisition on non-heated specimens belonging to hearths Rest1 and Rest2. The results of this simulation are presented in an equal-area projection plot, where the directions of the NRM and the remanent magnetisation acquired after each successive pTRM acquisition step are displayed—note their position in relation with each axis. Additionally, each stereogram is accompanied by a small bar plot showing the intensity of the magnetisation acquired in each axis after each step, providing insight into the evolution of the magnetisation throughout the process.

Results from the artificial TRM acquisition indicate that the calcareous substrate, whose NRM is close to zero, acquires a magnetisation parallel to the applied experimental field (-*z* axis) when subjected to temperatures of 500 °C. This value is similar in magnitude to those recorded on the upper layers of the hearths (0–2 cm) during their prehistoric firing. Maximum magnetisation values from archaeologically heated hearths reach 1.7E − 06 Am^2/kg (see 'Rock Magnetism and Magnetic Mineralogy' section and Fig. 4B), whilst the laboratory-induced TRM shows values between 1.56E − 06 and 5.94E − 06 Am^2/kg. Subsequent magnetisation at lower temperatures in different axes demonstrates that, although pTRM acquisition mechanisms are efficient at 400 °C and 450 °C (as evidenced by the equal-area plots for both specimens, which show very similar acquisition trajectories), they do not reach the same intensities as the first pTRM induced at 500 °C. The variation in magnetisation across each axis, shown in the bar graphs, indicates that the first pTRM acquired at 500 °C in the -*z* axis is progressively erased, whilst it increases in the -*y* axis.

The last step, which accounts for another change in the axis of magnetisation (-*x* at 350 °C), confirms that: (a) the materials are able to acquire a partial magnetisation along the axis where the field is applied, (b) the partial thermoremanence acquired at lower temperatures shows lower intensities, and (c) the pTRM acquired at 350 °C does not completely erase the pTRM previously imparted at 500 °C (the pTRM at 500 °C is fully removed only when higher temperatures are applied).

It is worth mentioning that the direction of the acquired pTRM does not perfectly align with the applied magnetic field at lower temperatures (e.g. at 350 °C), as the previous magnetisation in the other axes is not completely removed. Figure 5 shows how the direction of the magnetisation acquired at 350 °C is not completely parallel to the -*x* axis, and higher temperatures are required for full alignment in that direction. At 400 °C and 450 °C, the acquisition mechanism appears to be more efficient, with the TRM direction becoming closer to the -*y* axis. However, complete alignment with the laboratory field seems to be achieved only at 500 °C (or, potentially, higher temperatures).

Archaeomagnetism

The NRM of the four combustion structures shows a large dispersion (Fig. 6), albeit with a northward trend on average.

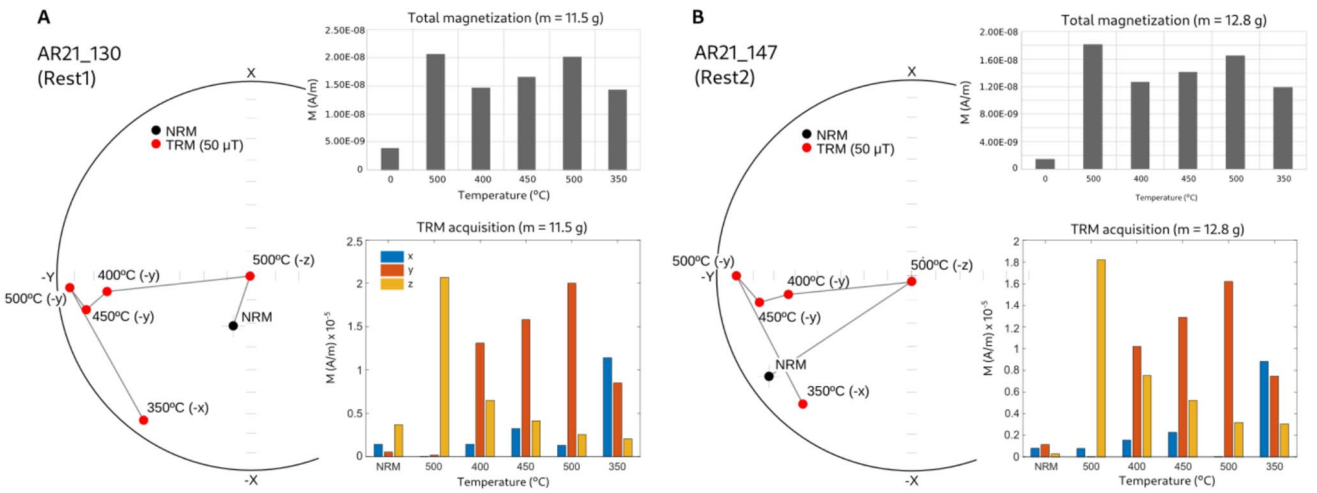

Fig. 5 Laboratory-induced fresh pTRM acquisition along all three orthogonal axes of two unburnt specimens in a field of 50 µT. The stereograph shows the different temperature steps and the axes along which the pTRM was imparted; the bar graphs show the total magnetisation acquisition (up) and the variation of the magnetisation in each axis (down)

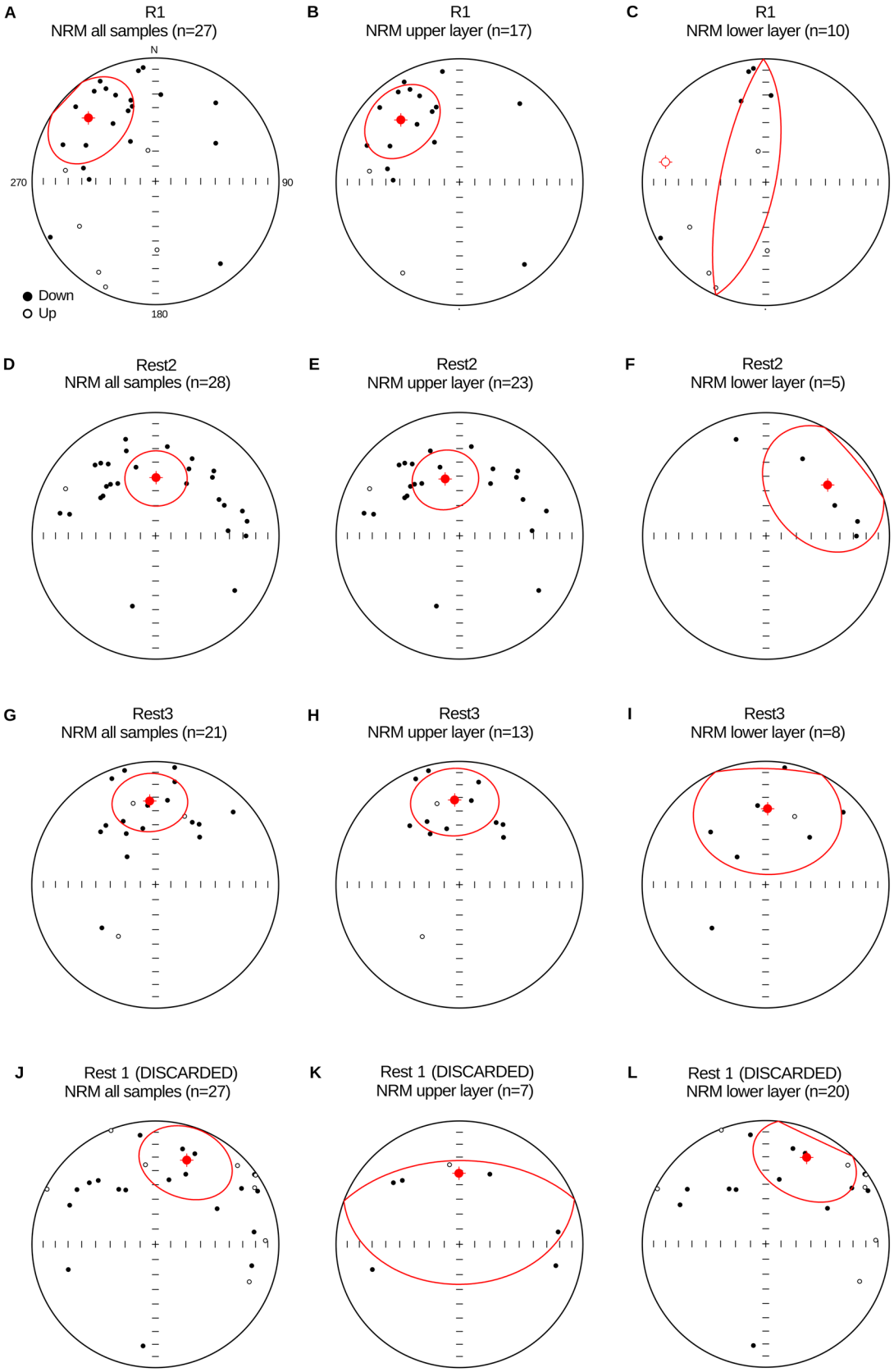
A
R1
NRM all samples (n=27)
N
270
90
180
Down
Up
B
R1
NRM upper layer (n=17)
C
R1
NRM lower layer (n=10)
D
Rest2
NRM all samples (n=28)
E
Rest2
NRM upper layer (n=23)
F
Rest2
NRM lower layer (n=5)
G
Rest3
NRM all samples (n=21)
H
Rest3
NRM upper layer (n=13)
I
Rest3
NRM lower layer (n=8)
J
Rest 1 (DISCARDED)
NRM all samples (n=27)
K
Rest 1 (DISCARDED)
NRM upper layer (n=7)
L
Rest 1 (DISCARDED)
NRM lower layer (n=20)

◂**Fig. 6** NRM distribution of all the studied specimens, grouped by its internal location within the hearth (upper vs. lower layers, as described above). **A**, **B**, **C** Hearth R1; **D**, **E**, **F** hearth Rest2; **G**, **H**, **I** hearth Rest3; **J**, **K**, **L** hearth Rest, whose higher dispersion prevented its use for directional calculations

Many specimens exhibit directions that are not consistent with the expected normal polarity record of the geomagnetic field during the estimated age of the hearths (*ca*. 60 ky BP). This suggests the potential syn- or post-depositional disturbances at macroscopic scales, and/or particle motion at a microscopic level due to fluid circulation in the karstic system and the high porosity of the materials. Alternatively, it is possible that some specimens did not reach a high enough temperature during heating to acquire a stable TRM. Further analysis of the variation of the NRM with depth shows that, for three of the four studied hearths, specimens belonging to the lower layers (2–4 cm below the surface) exhibit a greater dispersion (Fig. 6C, F, I) compared to those from the upper layers (0–2 cm below surface, Fig. 6B, E, H). This confirms the expectation that samples from the upper layer, which are in direct contact with fire and thus most heated, are more likely to acquire a stable partial TRM or pTCRM (thermochemical remanent magnetisation). In contrast, those from the lower layers, subjected to lesser heating effects, might not have reached sufficiently high temperatures to record the ancient geomagnetic field. These specimens, mostly from the lower layers, have thus been excluded from directional calculations.

Of all 106 demagnetised specimens, 74 exhibit erratic, 'unreadable' plots with no clear direction and were discarded (e.g. Figure 7G–I). In contrast, 32 out of 106 specimens show good remanence records (after cleaning the viscous component, which is present in every specimen sometimes up to 250 °C; the viscous component is not considered for directional analysis nor for discussion, as its imprint does not correspond to the Palaeolithic geomagnetic field). The results reveal two different behaviours:

- Specimens with two magnetic components (21.8%) exhibit: (a) a low-temperature *(LT)* component defined between 200 and 250 °C and 340–440 °C, which is very dispersed and shows random directions; and (b) a high temperature (*HT*) component defined between 400 °C and the complete demagnetisation at 500–600 °C (Fig. 7A, B, C, E), showing northward directions.
- Specimens with a single magnetic component labelled as LHT (low–high temperature, 71.8%) defined between 250 °C and 500–600 °C (Fig. 7D, F). This component exhibits northward directions.

In summary, 32 out of the initial 106 specimens studied provided reliable directional results (Table in Supplementary Information SI1). The HT or HLT components from hearts R1, Rest2, and Rest 3 were calculated with at least six temperature steps, and MAD angles < 20°. In contrast, almost all specimens from structure Rest1 exhibited erratic Zijderveld plots and/or anomalous and highly dispersed directions (Fig. 7G–I), indicating that they may have undergone reworking processes or other physical alterations; it thus has been excluded from further discussion.

The low (LT) and high (HT or LHT) temperature components of hearths R1, Rest2, and Rest3 and their means are represented separately in equal area plots in Fig. 8a–c. The high temperature component shows a good grouping and northward directions, whilst the low-temperature component appears to be highly scattered. As such, we have taken the high-temperature component (HT and LHT) as the characteristic remanent magnetisation (ChRM) that bears the last accurate record of the direction of the geomagnetic field at *ca.* 60 ky BP.

The mean ChRM directions of structures R1, Rest2, and Rest3 are reported in Table 2. For each hearth, between 9 and 13 specimens were used in the calculation. All the directions are northward and relatively well clustered, with α_{95} values of 10°, 9.7°, and 6.8°, respectively. The mean directions of hearths R1 and Rest2 are statistically indistinguishable; in contrast, hearth Rest3 shows a slightly different direction, approximately 20° or 30° to the east compared to the other two structures (Fig. 8d).

Discussion

Although previous works have explored hearths of approximately the same age (Carrancho et al., 2016; Herrejón-Lagunilla et al., 2024; Leierer et al., 2020; Zeigen et al., 2019), there is a notable scarcity of archaeomagnetic research focused on Middle Palaeolithic sites. This study addresses this gap by conducting rock-magnetic and archaeodirectional analyses of four Middle Palaeolithic hearths from the Abric Romaní (NE Spain).

Results from rock magnetism experiments reveal that the materials consist predominantly of diamagnetic minerals, although small amounts of magnetite are present in the uppermost centimetres below the surface of the hearths. The presence of magnetite and/or slightly oxidised magnetite is likely related to the magnetic enhancement resulting from fire, arising from the transformation of iron-bearing minerals in the fuel (McClean & Kean, 1993), or those previously present in the substrate. A similar mineralogy was also observed in previous archaeomagnetic studies conducted on hearths from Level O of the shelter (Carrancho et al., 2016). Nevertheless, the striking magnetic weakness in the studied hearths prompted us to explore whether the samples from Level R are prone to acquiring a stable thermoremanent

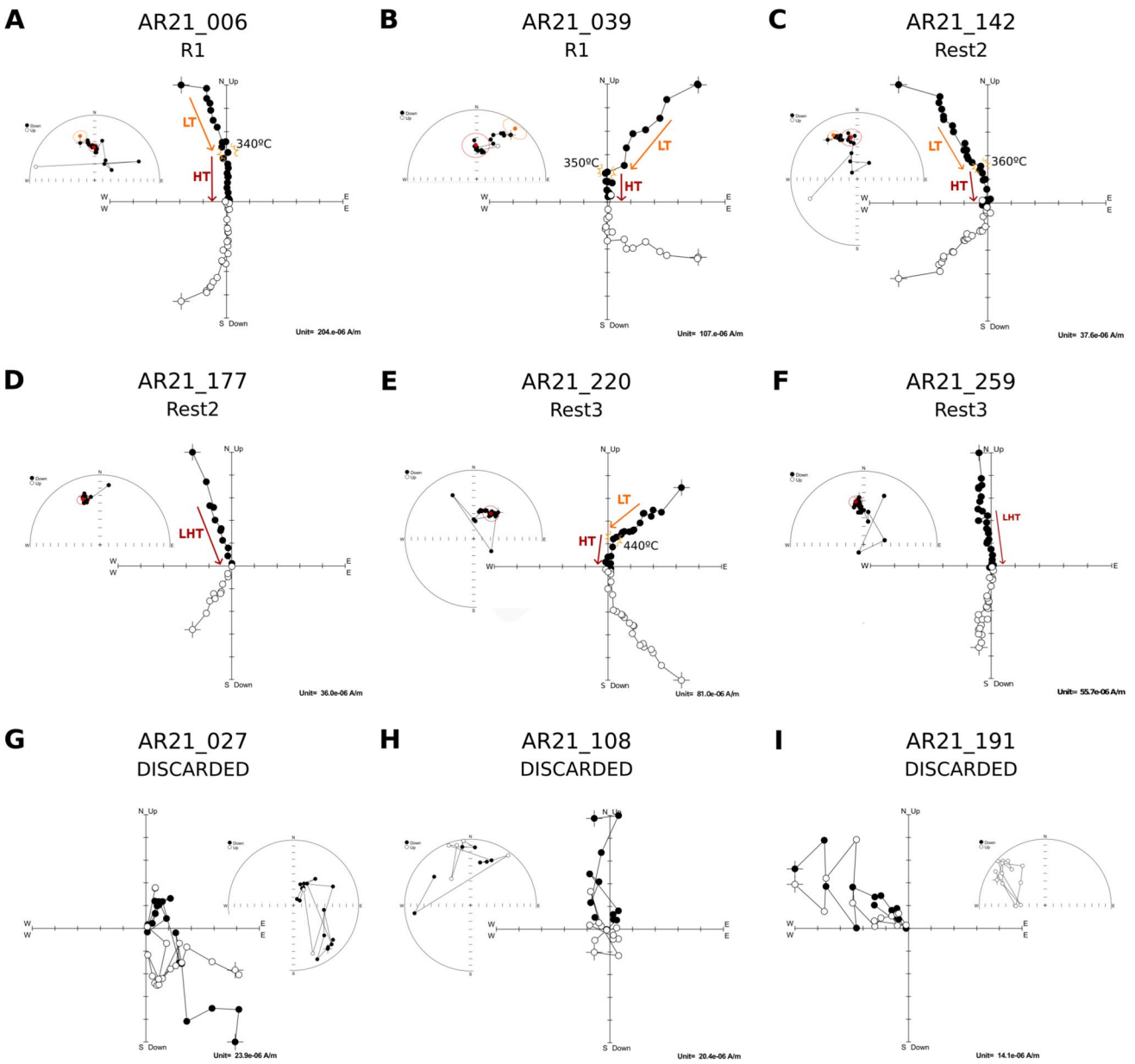

Fig. 7 Representative Zijderveld and equal-area plots for representative specimens: **A**, **B**, **C**, **E** with two components; **D**, **F** specimens with a single component; discarded specimens (**G**, **H**, **I**)

magnetisation under controlled heating conditions and a known artificial magnetic field.

Several samples from the calcareous, non-heated substrate were subjected to a laboratory-induced partial thermoremanent acquisition experiment along all three orthogonal axes in a field of 50 μT. The acquisition of the induced pTRMs occurs parallel to the axis along which the field is applied, and changes accordingly when the field is induced along another axis. This experiment further supports the hypothesis that the materials can acquire a pTRM parallel to an ambient field when heated to medium–high temperatures (450 °C or higher).

After stepwise thermal demagnetisation, the samples that exhibited erratic or unstable plots were excluded from further analysis. Of the four hearths analysed, three provided interpretable plots (R1, Rest2, Rest3). Data retrieved from Rest1 proved unsuitable, either because the hearth did not reach high enough temperatures during the burning process in the past, or because it sustained post-combustion erosional processes, reworking, or other physical alteration that removed its upper layer.

Upon the removal of the viscous component, the specimens show a high unblocking temperature (HT or LHT component, depending on whether they are

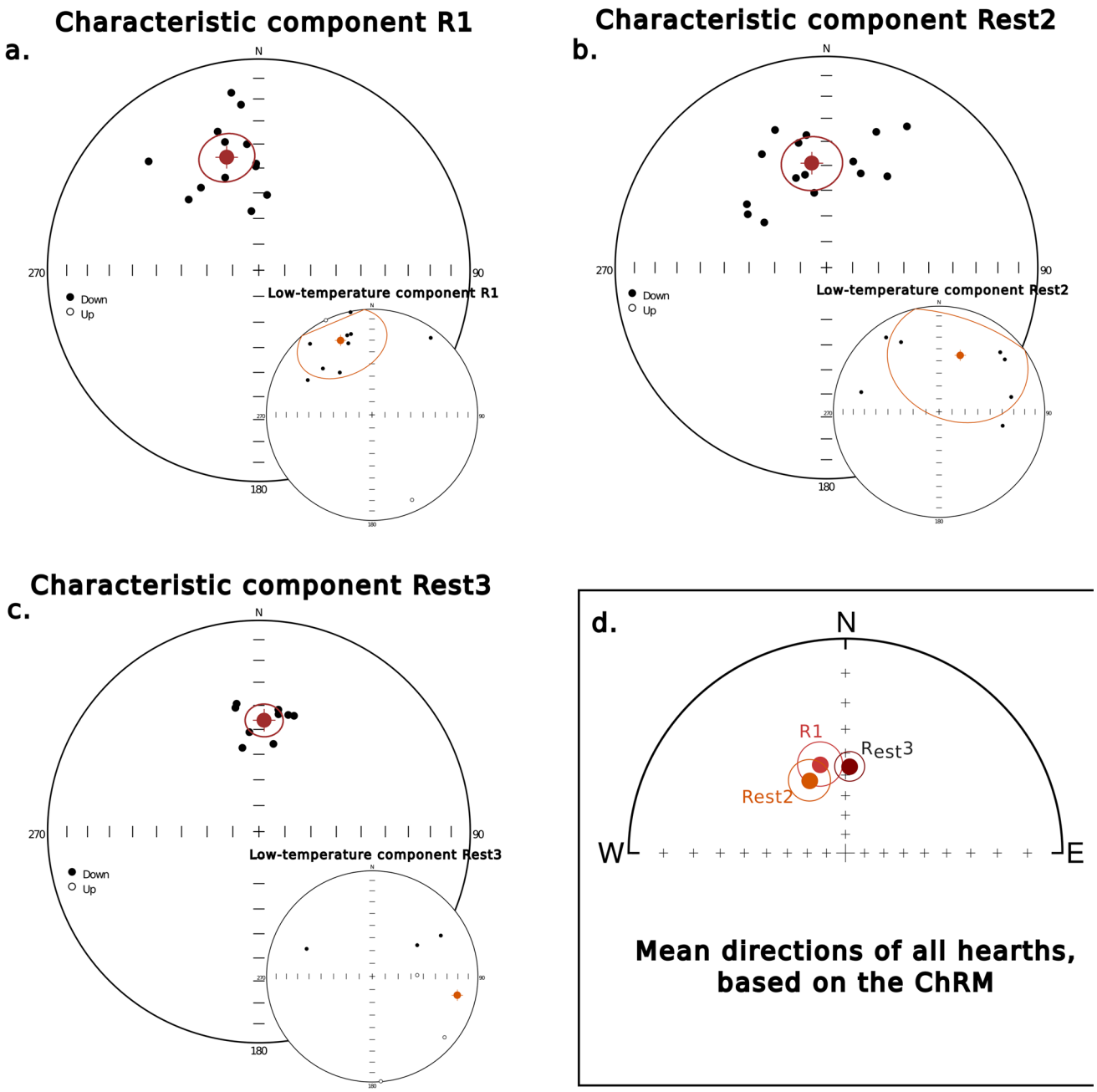

Fig. 8 **a**, **b**, **c** Directions of the ChRM (main equal-area projection) and low-temperature component (small inset) of the studied hearths; **d** mean directions of hearths R1, Rest2, and Rest3, calculated from the ChRM of each specimen

Table 2 ChRM mean directions of the three combustion structures. *n*, number of specimens used for calculation; *N*, total of specimens demagnetised; *N'*, number of hand field blocks; *DEC*, magnetic declination, in degrees; *INC*, magnetic inclination, in degrees; *k*, precision parameter; α_{95}, 95% cone of confidence, in degrees

Hearth	*n*	*N*	*N'*	DEC (°)	INC (°)	*k*	α_{95} (°)
AR21_R1_ChRM	13	28	3	344.2	43.7	18	10.0
AR21_Rest2_ChRM	10	28	5	333.9	48.9	26	9.7
AR21_Rest3_ChRM	9	28	2	2.7	46.1	59	6.8

single or multicomponent specimens), defined between 250- or 440 °C and 580 °C, and display consistent northward and well grouped directions. We consider this to be the ChRM, i.e. the component that recorded the direction of the geomagnetic field at 60 ky BP during a burning-and-cooling process. This is supported by the aforementioned artificial pTRM acquisition experiment, during which the magnetisation acquired by unburned specimens is similar in magnitude to the NRM of those used for the ChRM calculation. Additionally, the experiment proves that the calcareous substrate can acquire a well-defined pTRM, suggesting that the ChRM was acquired as a pTRM or pTCRM through heating to medium–high temperatures (at least 450 °C) during prehistoric times.

This behaviour is consistent with results from other Middle Palaeolithic sites—e.g. the interdisciplinary study of El Salt, in the east of the Iberian peninsula, by Leierer et al. (2020)—and agrees with previous data about temperatures reached by the carbonaceous black layers and underlying substrate of prehistoric fires in other studies (Carrancho et al., 2009, 2012, 2013; Herrejón-Lagunilla et al., 2022, 2024). The new data can complement other studies on Neanderthal pyrotechnology that consider fire intensity and its effects on the sedimentary deposits at Abric Romaní, such as those reported by Vallverdú and Courty (2012) for level J.

A low-temperature component (LT) is observed in several specimens between 220 and 250 °C and up to 420–440 °C. This shows neither a northern direction nor is it well-grouped or consistent amongst different specimens from the same hearth. It cannot be explained solely by a thermal acquisition process; instead, it may result from chemical or thermo-chemical processes acting locally at the centimetric scale. Different specimens from the same field sample show scattered directions for the LT component, whilst the HT northward component is consistently preserved. This observation aligns with the complex geological features occurring within the shelter, where sedimentation is heavily dominated by the chemical precipitation of calcium carbonate, including local dripping, and the disaggregation (weathering) of tufa deposits from the cliff and roof of the shelter—as reported in Vallverdú et al. (2012b). The random distribution of the LT component cannot be due to the mechanical remotion of the hearth; if it were, it would have affected the full vector. It is our opinion that the HT component represents an earlier burning event—one that accurately recorded the geomagnetic field—whilst the LT component corresponds to a more recent, lower temperature burning event, possibly coupled with a chemical or thermo-chemical process. Some experimental studies conducted in the 1980s demonstrated that a CRM or TCRM does not always accurately record the field's direction (Heider & Dunlop, 1987; Özdemir & Dunlop, 1985). This was observed in the magnetite-maghemite series, which is compatible with our results, that point to magnetite and/or maghemitised magnetite as the carrier of the magnetisation.

The directions obtained from all the discussed hearths (R1, Rest2, and Rest3) are consistent with the expected configuration of the geomagnetic field during their estimated age, *ca.* 60 ky BP. The three combustion structures provide northward and well grouped directions, with no significant statistical differences between two of them (R1 and Rest2). The overlapping between the confidence angle of structures R1 and Rest2 compels us to suggest that they belong to the same occupation episode at the rock shelter. A note of caution is in order, as already noted by others (Carrancho et al., 2016; Herrejón-Lagunilla et al., 2024; Zeigen et al., 2019): due to the cyclical nature of the regional changes in the geomagnetic field (the secular variation) and the repeating patterns of declination, inclination, and intensity throughout time, a more accurate statement would be that these hearths are not *categorically diachronic.* A synchronous use of these hearths cannot be fully posited, and the definitive attribution to a specific archaeological sub-level within the greater Level R must take into account other archaeological proxies—such as intra-site spatial analysis and charcoal and fuel analysis. Hearth Rest3 shows a slightly better directional grouping and does not share the same direction as the other two (Fig. 9). Although we cannot determine *when* this structure acquired its magnetisation—whether before or after the other two—we can suggest that the geomagnetic field was most likely recorded at a different time than in the other two structures. The classification of hearth Rest3 as *structural*—that is, one that cannot be definitively attributed to either of the known sub-levels of unit R (Fig. 1C)—supports the hypothesis of a different timing.

A side-to-side comparison of the mean directions from level O at the Abric Romaní (*ca.* 55 ky BP) by Carrancho et al. (2016) and those in this study (Level R, *ca.* 60 ky BP) shows that the older level R recorded more westerly directions (Fig. 9). Although no high-resolution palaeosecular variation curve for the Middle Palaeolithic in Iberia

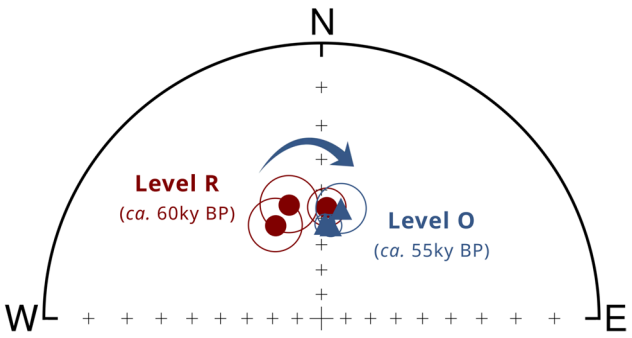

Fig. 9 Equal-area plot with the mean directions and confidence angles obtained in this study (maroon circles) and those from Carrancho et al. (2016) previous studies (blue triangles)

exists that would allow to compare our results, the available data, though limited, allow for a preliminary assessment of changes in the Earth's magnetic field direction. These new data points are not enough to make definitive claims about geomagnetic field changes between 60 and 55 ky BP, but they expand the available directional database for this period in NE Iberia. Broadening our understanding of the behaviour of the geomagnetic field at such ancient ages is, indeed, an exciting prospect.

The results reported above suggest a way forward for Palaeolithic archaeomagnetism whilst recognising its challenges. Perhaps the most prominent issue is the very low success rate of the experiments—the small number of specimens that produced clear and meaningful directional results. Another difficulty is the diamagnetic nature of the calcareous substrate material at Level R, which masks the faint signal from the ferromagnetic minerals responsible for the magnetisation. Building upon previous studies at the same site, we remain optimistic about the potential of these environments to provide a detailed characterisation of the prehistoric geomagnetic field. Archaeomagnetism has already proved useful in identifying human occupation linked to combustion structures, and even in dating them (Herrejón-Lagunilla et al., 2024). For this to be a widespread possibility, though, well-preserved in situ burned facies carrying an original ChRM must be identified. As this study shows, such conditions are not always fulfilled in Middle Palaeolithic hearths. Future research at the Romaní and similar sites should carefully consider sub-sampling procedures, and engage in a cautious analysis at the specimen level, as the hearths' surfaces can be altered differently in adjacent sections of the same hearth, even if the remanence was acquired during the same firing event. This work aims to contribute, on its own way, to our understanding of Neanderthal behaviours and lifestyles in temperate climates; and to highlight the potential of interdisciplinary archaeological research in decoding our remote past.

Conclusions

Following the results provided by rock magnetism and archaeomagnetic analyses in the Abric Romaní's level R, a few conclusions can be drawn:

- The primary carrier of magnetisation is a ferromagnetic mineral with low coercivity and unblocking temperatures around 580 °C, likely magnetite and/or slightly maghemitised magnetite.
- Archaeomagnetic and rock-magnetic analyses indicate that the hearths consistently reached temperatures of 350–450 °C or higher during their use, and that the calcareous substrate at the site shows reasonably good potential to acquire a partial thermoremanent or thermochemical magnetisation parallel to the ambient field.
- Three of the hearths successfully recorded the direction of the geomagnetic field *ca.* 60 ky BP. Most specimens show two components: a chaotic low-temperature component (resulting from secondary chemical or thermochemical processes) and a stable high-temperature component which was identified as the characteristic remanent magnetisation (ChRM). The remaining hearth was excluded from analysis, since its specimens showed erratic demagnetisation plots.
- Three new archaeomagnetic directions for the Middle Palaeolithic were obtained. The archaeomagnetic directions in Level R hearths (*ca.* 60 ky BP) differ from those previously studied belonging to the younger Level O at the same site (ca. 55 ky BP) at the same site.

Supplementary Information The online version contains supplementary material available at https://doi.org/10.1007/s41982-025-00213-6.

Acknowledgements The authors wish to acknowledge the support of the ArchaeologyHub.CSIC research network, as well as the two reviewer's comments and valuable suggestions. Thanks to Amanda Merino and Lila Warnitz for the updated cartography of the Abric Romaní's Level R. JdR expresses their gratitude to the archaeological team working on site at the Abric Romaní during the sampling of these materials, who provided help and much needed support.

Author Contribution JdR: Conceptualization, Validation, Formal Analysis, Investigation, Data Curation, Writing – original draft, Writing – review & editing, Visualization, Funding acquisition. AP-O: Conceptualization, Validation, Formal Analysis, Data Curation, Writing – original draft, Writing – review & editing, Visualization, Supervision. MG-P: Conceptualization, Validation, Formal Analysis, Resources, Data Curation, Writing – original draft, Writing – review & editing, Visualization, Supervision, Funding acquisition. AC: Conceptualization, Validation, Resources, Writing – review & editing, Visualization, Supervision, Funding acquisition. JV: Validation, Resources, Writing – review & editing, Visualization. PS: Validation, Resources. MGC: Validation, Resources, Writing – review & editing. EC: Validation, Resources.

Funding Open Access funding provided thanks to the CRUE-CSIC agreement with Springer Nature. This work was funded by the FPU20/03664 contract granted by the Spanish Ministry of Science, Innovation and Universities, the project PID2019105796GB-I00 of the Agencia Estatal de Investigación, Junta de Castilla y León, the European Regional Development Fund (project BU037P23), and Fundación PALARQ. Excavations at the Abric Romaní were carried out with the support of the Departament de Cultura of the Generalitat de Catalunya (ARQ001SOL-201–2022), Town Council of Capellades and Romanyà-Valls S.A, the SGR 2021 01237 (AGAUR), and the I+D+i project PID2022-138590NB-C41, funded by MCIN/AEI/https://doi.org/10.13039/501100011033and by the ERDF A way of making Europe. P.S., J.V. and M.G.Ch. research is funded by the CERCA Program (Generalitat de Catalunya).

Data Availability Data is provided within the manuscript and as a supplementary file. It can also be found at https://doi.org/10.5281/zenodo.12772590.

Declarations

Competing Interests The authors declare no competing interests.

References

Aldeias, V., Dibble, H. L., Sandgathe, D., Goldberg, P., & McPherron, S. J. P. (2016). How heat alters underlying deposits and implications for archaeological fire features: A controlled experiment. *Journal of Archaeological Science, 67*, 64–79. https://doi.org/10.1016/j.jas.2016.01.016

Allué, E., Cabanes, D., Solé, A., & Sala, R. (2012). Hearth functioning and forest resource exploitation based on the archeobotanical assemblage from Level J. In E. Carbonell i Roura (Ed.), *High resolution archaeology and Neanderthal behavior: Time and space in level J of Abric Romaní (Capellades, Spain)* (pp. 373–385). Springer Netherlands. https://doi.org/10.1007/978-94-007-3922-2_9

Allué, E., Mallol, C., Aldeias, V., Burguet-Coca, A., Cabanes, D., Carrancho, Á., Connolly, R., Leierer, L., Mentzer, S., Miller, C., Sandgathe, D., Stahlschmidt, M., Théry-Parisot, I., & Vaquero, M. (2022). Fire among Neanderthals. In F. Romagnoli, F. Rivals, & S. Benazzi (Eds.), *Updating Neanderthals* (pp. 227–249). Academic Press. https://doi.org/10.1016/B978-0-12-821428-2.00014-7

Álvarez-Fernández, E., Bécares, J., Jordá Pardo, Jesús F., Aguirre Uribesalgo, A., Álvarez-Alonso, D., de Andrés-Herrero, M., Aparicio Alonso, M. T., Barrera Mellado, I., Carral González, P., Carriol, R.-P., Chauvin Grandela, A. M., Cubas Morera, M., Cueto Rapado, M., Domingo, R., Douka, K., Duarte, C., Elorza Espolosin, M., Fernández Gómez, M. J., Gabriel, S., & Arias Cabal, P. (2018). La cueva de El Cierro (Frusnu, Ribadesella). Campañas de excavación e investigación 1977–1979, 2014 y 2016. In *Excavaciones arqueológicas en Asturias. 2013–2016*. Consejería de Educación y Cultura. Gobierno del Principado de Asturias.

Bailey, G. (2007). Time perspectives, palimpsests and the archaeology of time. *Journal of Anthropological Archaeology, 26*(2), 198–223. https://doi.org/10.1016/j.jaa.2006.08.002

Bischoff, J., Julia, R., Mora, R. (1988). Uranium-series dating of the Mousterian occupation at the Abric Romani, Spain. *Nature, 332*, 68e70.

Bonilla-Alba, R. et al. (2024). First full-vector archeomagnetic data from Central Asia (3 BCE to 15 CE centuries): Evidence for a large non-dipole field contribution around the first century BCE. *Journal of Geophysical Research: Solid Earth*, *129*(2), e2023JB027910. https://doi.org/10.1029/2023JB027910

Bonilla-Alba, R., Gómez-Paccard, M., Pavón-Carrasco, F.J., del Río, J., Beamud, E., Martínez-Ferreras, V., Gurt-Esparraguera, J.M., Ariño-Gil, A., Palencia-Ortas, A., Martín-Hernández, F., Chauvin, A., & Osete, M.L. (2021). Rapid intensity decrease during the second half of the first millennium BCE in Central Asia and global implications. *Journal of Geophysical Research, Solid Earth, 126*, e2021JB022011. https://doi.org/10.1029/2021JB022011

Bradák, B., Carrancho, Á., Herrejón Lagunilla, Á., Villalaín, J. J., Monnier, G. F., Tostevin, G., Mallol, C., Pajović, G., Baković, M., & Borovinić, N. (2021). Magnetic fabric and archaeomagnetic analyses of anthropogenic ash horizons in a cave sediment succession (Crvena Stijena site, Montenegro). *Geophysical Journal International, 224*(2), 795–812. https://doi.org/10.1093/gji/ggaa461

Brown, K. S., Marean, C. W., Herries, A. I. R., Jacobs, Z., Tribolo, C., Braun, D., Roberts, D. L., Meyer, M. C., & Bernatchez, J. (2009). Fire as an engineering tool of early modern humans. *Science, 325*(5942), 859–862. https://doi.org/10.1126/science.1175028

Brown, M. C., Hervé, G., Korte, M., & Genevey, A. (2021). Global archaeomagnetic data: The state of the art and future challenges. *Physics of the Earth and Planetary Interiors, 318*, 106766. https://doi.org/10.1016/j.pepi.2021.106766

Campuzano, S. A., Gómez-Paccard, M., Pavón-Carrasco, F. J., & Osete, M. L. (2019). Emergence and evolution of the South Atlantic Anomaly revealed by the new paleomagnetic reconstruction SHWQ2k. *Earth and Planetary Science Letters, 512*, 17–26. https://doi.org/10.1016/10.1016/j.epsl.2019.01.050

Carrancho, Á., Villalaín, J. J., Angelucci, D. E., Dekkers, M. J., Vallverdú, J., & Vergès, J. M. (2009). Rock-magnetic analyses as a tool to investigate archaeological fired sediments: A case study of Mirador cave (Sierra de Atapuerca, Spain). *Geophysical Journal International, 179*(1), 79–96. https://doi.org/10.1111/j.1365-246X.2009.04276.x

Carrancho, Á., Villalaín, J. J., Vergès, J. M., & Vallverdú, J. (2012). Assessing post-depositional processes in archaeological cave fires through the analysis of archaeomagnetic vectors. *Quaternary International*. https://doi.org/10.1016/j.quaint.2012.01.010

Carrancho, Á., Villalaín, J. J., Pavón-Carrasco, F. J., Osete, M. L., Straus, L. G., Vergès, J. M., Carretero, J. M., Angelucci, D. E., González Morales, M. R., Arsuaga, J. L., Bermúdez de Castro, J. M., & Carbonell, E. (2013). First directional European palaeosecular variation curve for the Neolithic based on archaeomagnetic data. *Earth and Planetary Science Letters, 380*, 124–137. https://doi.org/10.1016/j.epsl.2013.08.031

Carrancho, Á., Villalaín, J. J., Vallverdú, J., & Carbonell, E. (2016). Is it possible to identify temporal differences among combustion features in Middle Paleolithic palimpsests? The archaeomagnetic evidence: A case study from level O at the Abric Romaní rock-shelter (Capellades, Spain). *Quaternary International, 417*, 39–50. https://doi.org/10.1016/J.QUAINT.2015.12.083

Chadima, M., & Hrouda, F. (2006). Remasoft 3.0 – A user-friendly paleomagnetic data browser and analyzer. *Travaux Géophysiques*, *27*, 20–21. http://hdl.handle.net/11104/0140618. Accessed 05/03/2025

Courty, M.-A., Carbonell, E., Vallverdú Poch, J., & Banerjee, R. (2012). Microstratigraphic and multi-analytical evidence for advanced Neanderthal pyrotechnology at Abric Romani (Capellades, Spain). *Quaternary International, 247*, 294–312. https://doi.org/10.1016/j.quaint.2010.10.031

Di Chiara, A., Tauxe, L., Levy, T. E., Najjar, M., Florindo, F., & Ben-Yosef, E. (2021). The strength of the Earth's magnetic field from Pre-Pottery to Pottery Neolithic, Jordan. *Proceedings of the National Academy of Sciences, 118*(34), e2100995118. https://doi.org/10.1073/pnas.2100995118

Dibble, H. L., Sandgathe, D., Goldberg, P., McPherron, S., & Aldeias, V. (2018). Were Western European Neandertals able to make fire?

Journal of Paleolithic Archaeology, 1(1), 54–79. https://doi.org/10.1007/s41982-017-0002-6

Dinçkal, A., Carrancho Alonso, A., Hernandez Gomez, C. M., & Mallol, C. (2024). Magnetic micro-archaeology: A method for conducting rock magnetic microfacies analysis on archaeological soil micromorphology samples, with a case study from El Salt, Alcoy Spain. *Archaeological and Anthropological Sciences, 16*(3), 44. https://doi.org/10.1007/s12520-024-01946-1

Fisher, R. A. (1953). Dispersion on a sphere. *Proceedings of the Royal Society of London, 217*(1130), 295–305. https://doi.org/10.1098/rspa.1953.0064

Francés-Negro, M., Carrancho, Á., Pérez-Romero, A., Arsuaga, J. L., Carretero, J. M., & Iriarte, E. (2019). Storage or cooking pots? Inferring pottery use through archaeomagnetic assessment of palaeotemperatures. *Journal of Archaeological Science, 110*, 104992. https://doi.org/10.1016/j.jas.2019.104992

Gallet, Y., Genevey, A., Le Goff, M., Warmé, N., Gran-Aymerich, J., & Lefèvre, A. (2009). On the use of archeology in geomagnetism, and vice-versa: Recent developments in archeomagnetism. *Comptes Rendus Physique, 10*(7), 630–648. https://doi.org/10.1016/j.crhy.2009.08.005

Gómez-Paccard, M., Rivero-Montero, M., Chauvin, A., García i Rubert, D., & Palencia-Ortas, A. (2019). Revisiting the chronology of the Early Iron Age in the north-eastern Iberian Peninsula. *Archaeological and Anthropological Sciences, 11*(9), 4755–4767. https://doi.org/10.1007/s12520-019-00812-9

Heider, F., & Dunlop, D. J. (1987). Two types of chemical remanent magnetization during the oxidation of magnetite. *Physics of the Earth and Planetary Interiors, 46*(1–3), 24–45. https://doi.org/10.1016/0031-9201(87)90169-5

Herrejón-Lagunilla, Á., Villalaín, J. J., Pavón-Carrasco, F. J., Serrano, M., Sossa-Ríos, S., Mayor, A., Galván, B., Hernández, C. M., Mallol, C., & Alonso, Á. C. (2024). The time between Paleolithic hearths. *Nature*. https://doi.org/10.1038/s41586-024-07467-0

Herrejón-Lagunilla, Á., Carrancho, Á., & Villalaín, J. J. (2022). On the suitability of prehistoric anthropogenic burnt sediments (fumiers) for archeomagnetic studies at El Mirador Cave (Burgos, Spain). In E. Allué, P. Martín, & J. M. Vergès (Eds.), *Prehistoric herders and farmers: A transdisciplinary overview to the archeological record from El Mirador Cave* (pp. 111–128). Springer International Publishing. https://doi.org/10.1007/978-3-031-12278-1_6

IPHES - Institut Català de Paleoecologia Humana i Evolució Social. (2020). *Memòria d'excavació programada Abric Romaní 2019–20*. IPHES (Institut Català de Paleoecologia Humana i Evolució Social).

IPHES - Institut Català de Paleoecologia Humana i Evolució Social. (2021). *Memòria d'excavació programada Abric Romaní 2021*. IPHES (Institut Català de Paleoecologia Humana i Evolució Social).

IPHES - Institut Català de Paleoecologia Humana i Evolució Social. (2022). *Memòria d'excavació programada Abric Romaní 2022*. IPHES (Institut Català de Paleoecologia Humana i Evolució Social).

Kapper, K. L., Anesin, D., Donadini, F., Angelucci, D. E., Cavulli, F., Pedrotti, A., & Hirt, A. M. (2014). Linking site formation processes to magnetic properties. Rock- and archeomagnetic analysis of the combustion levels at Riparo Gaban (Italy). *Journal of Archaeological Science, 41*, 836–855. https://doi.org/10.1016/j.jas.2013.10.015

Kapper, K. L., Donadini, F., & Hirt, A. M. (2015). Holocene archeointensities from mid European ceramics, slags, burned sediments and cherts. *Physics of the Earth and Planetary Interiors, 241*, 21–36. https://doi.org/10.1016/j.pepi.2014.12.006

Kirschvink, J. L. (1980). Principal component analysis of palaeomagnetic directions: Converting a Maximum Angular Deviation (MAD) into an α95 angle. *Geophysical Journal International, 62*(3), 699–718. https://doi.org/10.1111/j.1365-246X.1980.tb02601.x

Koenigsberger, J.G. (1930). Größenverhältnis von remanentem zu induziertem Magnetismus in Gesteinen; Größe und Richtung des remanenten Magnetismus. *Zeitschrift für Geophysik*, *6*, 190–207. https://doi.org/10.23689/fidgeo-3212

Kostadinova-Avramova, M., Kovacheva, M., Boyadzhiev, Y., & Hervé, G. (2020). Archaeomagnetic knowledge of the Neolithic in Bulgaria with emphasis on intensity changes. *Geological Society, London, Special Publications, 497*(1), 89–111. https://doi.org/10.1144/SP497-2019-48

Le Goff, M., Gallet, Y., Genevey, A., & Warmé, N. (2002). On archeomagnetic secular variation curves and archeomagnetic dating. *Physics of the Earth and Planetary Interiors, 134*(3), 203–211. https://doi.org/10.1016/S0031-9201(02)00161-9

Leierer, L., Alonso, Á. C., Pérez, L., Herrejón Lagunilla, Á., Herrera-Herrera, A. V., Connolly, R., Jambrina-Enríquez, M., Hernández Gómez, C. M., Galván, B., & Mallol, C. (2020). It's getting hot in here – Microcontextual study of a potential pit hearth at the Middle Paleolithic site of El Salt. *Spain. Journal of Archaeological Science, 123*, 105237. https://doi.org/10.1016/j.jas.2020.105237

Leonhardt, R. (2006). Analyzing rock magnetic measurements: The RockMagAnalyzer 1.0 software. *Computers & Geosciences*, *32*(9), 1420–1431. https://doi.org/10.1016/j.cageo.2006.01.006

Lowrie, W. (1990). Identification of ferromagnetic minerals in a rock by coercivity and unblocking temperature properties. *Geophysical Research Letters, 17*(2), 159–162. https://doi.org/10.1029/GL017i002p00159

Mallol, C., Mentzer, S. M., & Miller, C. E. (2017). Combustion features. In *Archaeological soil and sediment micromorphology* (pp. 299–330). John Wiley & Sons, Ltd. https://doi.org/10.1002/9781118941065.ch31

Mallol, C., Hernández, C., Mercier, N., Falguères, C., Carrancho, Á., Cabanes, D., & Galván, B. (2019). Fire and brief human occupations in Iberia during MIS 4: Evidence from Abric del Pastor (Alcoy, Spain). *Scientific reports, 9*(1), 18281. https://doi.org/10.1038/s41598-019-54305-9

McClean, R. G., & Kean, W. F. (1993). Contributions of wood ash magnetism to archaeomagnetic properties of fire pits and hearths. *Earth and Planetary Science Letters, 119*, 387–394. https://doi.org/10.1016/0012-821X(93)90146-Z

Moskowitz, B. M. (1981). Methods for estimating Curie temperatures of titanomaghemites from experimentalJs-T data. *Earth and Planetary Science Letters, 53*(1), 84–88. https://doi.org/10.1016/0012-821X(81)90028-5

Néel, L. (1955). Some theoretical aspects of rock-magnetism. *Advances in Physics, 4*(14), 191–243. https://doi.org/10.1080/00018735500101204

Néel, L. (1949). Théorie du traînage magnétique des ferromagnétiques en grains fins avec application aux terres cuites. *Annales de Géophysique*, *5*, 99–136. https://hal.science/hal-03070532/

Özdemir, Ö., & Dunlop, D. J. (1985). An experimental study of chemical remanent magnetizations of synthetic monodomain titanomaghemites with initial thermoremanent magnetizations. *Journal of Geophysical Research: Solid Earth, 90*(B13), 11513–11523. https://doi.org/10.1029/JB090iB13p11513

Palencia-Ortas, A., Molina-Cardín, A., Osete, M. L., Gómez-Paccard, M., Martín-Hernández, F., Chauvin, A., & Roperch, P. (2021). Inclination flattening effect in highly anisotropic archaeological structures from Iberia. Influence on archaeomagnetic dating. *Physics of the Earth and Planetary Interiors*, *318*, 106762. https://doi.org/10.1016/j.pepi.2021.106762

Pastó, I., Allué, E., & Vallverdu, J. (2000). Mousterian hearths at Abric Romaní, Catalonia (Spain). In C. Stringer, N. Barton, & C. Finlayson (Eds.), *Neanderthals on the Edge: Papers form a conference*

marking the 150th anniversary of the Forbes' Quarry discovery, Gibraltar. Oxbow Books.

Pavón-Carrasco, F. J., Rodríguez-González, J., Osete, M. L., & Torta, J. M. (2011). A Matlab tool for archaeomagnetic dating. *Journal of Archaeological Science, 38*(2), 408–419. https://doi.org/10.1016/j.jas.2010.09.021

Sandgathe, D. M., Dibble, H. L., Goldberg, P., McPherron, S. P., Turq, A., Niven, L., & Hodgkins, J. (2011). Timing of the appearance of habitual fire use. *Proceedings of the National Academy of Sciences, 108*(29), E298–E298. https://doi.org/10.1073/pnas.1106759108

Schmidt, A. (2007). Archeology, magnetic methods. In D. Gubbins & E. Herrero-Bervera (Eds.), *Encyclopedia of geomagnetism and paleomagnetism* (pp. 23–31). Springer Netherlands. https://doi.org/10.1007/978-1-4020-4423-6_9

Sharp, W. D., Mertz-Kraus, R., Vallverdu, J., Vaquero, M., Burjachs, F., Carbonell, E., & Bischoff, J. L. (2016). Archeological deposits at Abric Romaní extend to 110 ka: U-series dating of a newly cored, 30 meter-thick section. *Journal of Archaeological Science: Reports, 5*, 400–406. https://doi.org/10.1016/j.jasrep.2015.12.015

Stillinger, M. D., Feinberg, J. M., Ben-Yosef, E., Shaar, R., Hardin, J. W., & Blakely, J. A. (2018). A rejoinder on the value of archaeomagnetic dating: Integrative methodology is the key to addressing levantine iron age chronology. *Near Eastern Archaeology, 81*(2), 141–144. https://doi.org/10.5615/neareastarch.81.2.0141

Tarling, D. D. (2007). Archeomagnetism. In D. Gubbins & E. Herrero-Bervera (Eds.), *Encyclopedia of geomagnetism and paleomagnetism* (pp. 31–32). Springer Netherlands. https://doi.org/10.1007/978-1-4020-4423-6_10

Tauxe, L., Banerjee, S. K., Butler, R. F., & van der Voo, R. (2018). *Essentials of paleomagnetism: 5th Web Edition*.

Téllez, E., Saladié, P., Pineda, A., Marín, J., Vallverdú, J., Chacón, M. G., & Carbonell, E. (2022). Incidental burning on bones by Neanderthals: The role of fire in the Qa level of Abric Romaní rock-shelter (Spain). *Archaeological and Anthropological Sciences, 14*(6), 119. https://doi.org/10.1007/s12520-022-01577-4

Thellier, E. (1951). Propriétés magnétiques des terres cuites et des roches. *Journal De Physique Et Le Radium, 12*(3), 205–218. https://doi.org/10.1051/jphysrad:01951001203020500

Thellier, E. (1981). Sur la direction du champ magnétique terrestre, en France, durant les deux derniers millénaires. *Physics of the Earth and Planetary Interiors, 24*(2–3), 89–132. https://doi.org/10.1016/0031-9201(81)90136-9

Thellier, E., & Thellier, O. (1941). Sur les variations thermiques de l'aimantation thermorémanente des terres cuites. *Comptes Rendus De L'académie des Sciences (Paris), 213*, 59–61.

Thellier, E., & Thellier, O. (1959). Sur l'intensité du champ magnétique terrestre dans le passé historique et géologique. *Annales Geophysicae, 15*, 285–376.

Vallverdú, J. (2002). *Micromorfología de las facies sedimentarias de la colección de referencia de la Sierra de Atapuerca y del nivel J del Abric Romaní*. Universitat Rovira i Virgili.

Vallverdú, J., Allué, E., Bischoff, J. L., Cáceres, I., Carbonell, E., Cebrià, A., García-Antón, D., Huguet, R., Ibáñez, N., Martínez, K., Pastó, I., Rosell, J., Saladié, P., & Vaquero, M. (2005). Short human occupations in the Middle Paleolithic level i of the Abric Romaní rock-shelter (Capellades, Barcelona, Spain). *Journal of Human Evolution, 48*(2), 157–174. https://doi.org/10.1016/j.jhevol.2004.10.004

Vallverdú, J., Vaquero, M., Cáceres, I., Allué, E., Rosell, J., Saladié, P., Chacón, G., Ollé, A., Canals, A., Sala, R., Courty, M. A., & Carbonell, E. (2010). Sleeping activity area within the site structure of archaic human groups: Evidence from Abric Romaní Level N combustion activity areas. *Current Anthropology, 51*(1), 137–145. https://doi.org/10.1086/649499

Vallverdú, J., & Courty, M.-A. (2012). Microstratigraphic analysis of level J deposits: A dual paleoenvironmental-paleoethnographic contribution to Paleolithic archeology at the Abric Romaní. In E. Carbonell i Roura (Ed.), *High resolution archaeology and Neanderthal behavior: Time and space in level J of Abric Romaní (Capellades, Spain)* (pp. 77–133). Springer Netherlands. https://doi.org/10.1007/978-94-007-3922-2_4

Vallverdú, J., Alonso, S., Bargalló, A., Bartrolí, R., Campeny, G., Carrancho, Á., Expósito, I., Fontanals, M., Gabucio, J., Gómez, B., Prats, J. M., Sañudo, P., Solé, À., Vilalta, J., & Carbonell, E. (2012a). Combustion structures of archaeological level O and mousterian activity areas with use of fire at the Abric Romaní rockshelter (NE Iberian Peninsula). *Quaternary International, 247*, 313–324. https://doi.org/10.1016/j.quaint.2010.12.012

Vallverdú, J., Gómez de Soler, B., Vaquero, M., & Bischoff, J. L. (2012b). The Abric Romaní site and the Capellades region. In E. Carbonell i Roura (Ed.), *High resolution archaeology and Neanderthal behavior: Time and space in level J of Abric Romaní (Capellades, Spain)* (pp. 19–46). Springer Netherlands. https://doi.org/10.1007/978-94-007-3922-2_2

Vallverdú, J. (2018). Investigación geoarqueológica en los depósitos de ocupación musterienses del Pleistoceno superior del Abric Romaní (Capellades, Barcelona, España). *Boletín Geológico y Minero, 1129*(1–2), 129–152. https://doi.org/10.21701/bolgeomin.129.1.006

Vaquero, M., & Pastó, I. (2001). The definition of spatial units in Middle Paleolithic sites: The hearth-related assemblages. *Journal of Archaeological Science, 28*(11), 1209–1220. https://doi.org/10.1006/jasc.2001.0656

Vaquero, M., Allué, E., Bischoff, J. L., Burjachs, F., & Vallverdú, J. (2013). Environmental, depositional and cultural changes in the Upper Pleistocene and Early Holocene: the Cinglera del Capelló sequence (Capellades, Spain). Quaternaire. *Revue de l'Association française pour l'étude du Quaternaire, 24*(1), 49–64. https://doi.org/10.4000/quaternaire.6481

Wang, Q., Gong, Z., Victor, S. K., Corolla, M., Underhill, A. P., McIntosh, R. J., Fang, H., Ding, J., Zhao, Y., Chen, X., & Song, Y. (2023). New archaeomagnetic directions from Late Neolithic sites in Shandong province China. *Geophysical Journal International, 232*(2), 1159–1172. https://doi.org/10.1093/gji/ggac381

Zeigen, C., Shaar, R., Ebert, Y., & Hovers, E. (2019). Archaeomagnetism of burnt cherts and hearths from Middle Paleolithic Amud Cave, Israel: Tools for reconstructing site formations processes and occupation history. *Journal of Archaeological Science, 107*, 71–86. https://doi.org/10.1016/j.jas.2019.05.001